

Jenna Mehto

ABOUT METHODS TO CALCULATE CONTRALATERAL TEMPERATURE DIFFERENCES OF LOWER LIMBS

Bachelor's thesis
Faculty of Medicine and Health Technology
Instructor: Juha Hämäläinen
Inspector: Jari Viik
04/2023

TIIVISTELMÄ

Jenna Mehto: About the methods to calculate contralateral temperature differences of lower limbs (suomeksi: Alaraajalämpötilojen puolierolaskennan menetelmistä)

Kandidaatin tutkielma

Tampereen yliopisto

Bioteknologian ja biolääketieteen tekniikan koulutusohjelma

04/2023

Diabetes on maailmanlaajuisesti yksi merkittävimmistä sairauksista, sillä maailman diabetesliitto (International Diabetes Federation) on arvioinut diabetesta sairastavien määrän kasvavan merkittävästi vuoteen 2045 mennessä. Diabetes voidaan määritellä joukoksi sairauksia, joille ominaista on hyperglykemia eli korkea verensokeri johtuen glukoosiaineenvaihdunnan häiriöistä. Hyperglykemia johtuu keho kyvyttömyydestä käyttää tai tuottaa insuliinia alentamaan kehon verensokeria. Insuliinin riittämättömyydestä johtuen sairaus edellyttää veren glukoosipitoisuuden säännöllistä mittaamista mahdollisten komplikaatioiden ennaltaehkäisemiseksi.

Diabetekseen liittyvät jalkojen krooniset haavaumat ovat yksi merkittävimmistä diabeteksen komplikaatioista. Nämä vaikeahoitoiset jalkojen haavaumat altistavat diabetesta sairastavan alaraaja-amputaatioille. Jalkojen kroonisten haavaumien syntyminen on monissa tapauksissa ennaltaehkäistävissä huolehtimalla jalkojen hyvästä hoidosta. Kroonisten jalkahaavojen muodostumista voidaan ennaltaehkäistä myös alaraajalämpötilojen puolieron tarkastelun avulla, sillä tulehdus jalassa kohottaa ihon lämpötilaa tulehdusalueella.

Alaraajalämpötilojen puolieroa voidaan tarkastella lämpökamerakuvantamisen avulla. Lämpökamerakuvantaminen on ei-invasiivinen kuvantamismenetelmä, missä infrapunasäteilyä hyödynnetään kehon eri osien pintalämpötilajakauman tarkasteluun. Koska menetelmän avulla saadaan tietoa kehon fysiologisista prosesseista, voidaan menetelmällä tunnistaa kroonisten jalkahaavaumiin liittyviä tekijöitä.

Tämän tutkimuksen tarkoituksena oli analysoida lämpökamerakuvantamisen ohjelmistoa analysoimalla ohjelmiston virhekoodeja ja optimoimalla parametreja. Tutkimuksessa keskityttiin lämpökamerakuvantamisen puolierolaskentaan ja sen algoritmeihin. Puolierolaskennassa ohjelmisto muodostaa laskennan alaraajalämpötilojen puolierosta ja muodostaa tuloksen, joka indikoi alaraajojen välillä olevan mahdollisen puolieron. Tutkimus suoritettiin alustamalla parametriarvoja virhekoodeihin liittyville parametreille testausympäristössä. Luotu testausympäristö tuotti prosessin vaiheista tuloksena kuvaajan, joita arvioitiin tutkimuksessa.

Tutkimustulokset osoittavat, että tutkitut parametrit vaikuttavat lämpökamerakuvantamisen kuvankäsittelyyn ja parametrien optimoinnin avulla lämpökamerakuvantamisen kuvankäsittely voidaan optimoida. Tuloksien perusteella voitiin tunnistaa myös eri parametreihin liittyviä tekijöitä, jotka tulisi ottaa huomioon parametrien optimaalisia oletusarvoja suunniteltaessa.

Avainsanat: diabetes, jalkojen krooniset haavaumat, lämpökamerakuvantaminen, algoritmit, kuvankäsittely

Tämän julkaisun alkuperäisyys on tarkastettu Turnitin OriginalityCheck –ohjelmalla.

ABSTRACT

Jenna Mehto: About the methods to calculate contralateral temperature differences of lower limbs

Bachelor's thesis

Tampere University

Biotechnology and Biomedical Engineering, BSc (Tech)

04/2023

Diabetes is considered one of the most significant health issues globally and the International Diabetes Federation has estimated that the rise in the prevalence of diabetes will be prominent. Diabetes can be defined as a set of conditions in which glucose metabolism is affected. The characteristic hyperglycemia, defined as high blood glucose, is caused by the inability of the body to use, or produce insulin. The self-monitoring of blood glucose is required to decrease the risk of complications of the condition.

Diabetic foot ulceration is one of the major complications of diabetes in which the feet are affected by wounds. Due to this, they pose a risk of lower limb amputations. As the occurrence of diabetic foot ulcers is preventable in most cases and due to the raised skin temperatures in the areas of inflammation, the contralateral temperature differences can be utilized to predict the development of diabetic foot ulcers.

These contralateral temperature differences can be detected by utilizing infrared thermography. Infrared thermography is a non-invasive method of medical imaging in which infrared radiation is utilized to study the temperature distribution of the body surface. As the method provides information about the physiological processes of the human body, the factors often prevalent in diabetic foot ulceration can be recognized with infrared thermography.

The thesis focuses on analyzing the functioning of the infrared thermography software by analyzing the foundations of error codes and optimizing the parameters of the software. The focus was on the contralateral temperature difference calculations of the infrared thermography software. The contralateral temperature difference calculations aim to conduct the image processing and produce a result in which the possible contralateral temperature difference is indicated. To assess the foundations of the error codes, different parameter values for studied parameters associated with the error codes were tested in a created test environment. The test environment displayed an outcome from each step which was assessed in the thesis.

Based on the results acquired, the image processing of the infrared thermography software is influenced by the studied parameters and the optimal functioning of the algorithms could be achieved by optimizing the parameters associated with specific steps of the process. The thesis also identified complexities that need to be taken into consideration when finding optimal default values for parameters.

Keywords: diabetes, diabetic foot ulceration, infrared thermography, algorithms, image processing,

The originality of this thesis has been checked using the Turnitin OriginalityCheck service.

CONTENTS

1.INTRODUCTION	1
2.DIABETES AND ITS COMPLICATIONS.....	2
2.1 Types of diabetes	2
2.2 Diabetic neuropathy.....	3
2.3 Peripheral vascular disease.....	4
3.INFRARED THERMOGRAPHY IN DIABETIC FOOT ULCERATION	5
3.1 Overview of infrared thermography	5
3.2 Medical infrared thermography	6
3.3 Diabetic ulcer imaging	7
4.METHODS.....	8
4.1 Overview.....	8
4.2 Image segmentation	9
4.3 Symmetry and correspondence calculations	10
4.3.1 Calculations between feet in visual images	10
4.3.2 Calculations between thermal and visual feet.....	11
4.4 Temperature differences.....	12
4.5 Inspection of the parameters	12
4.5.1 Approximate offset.....	13
4.5.2 Contralateral correspondence area coverage.....	13
4.5.3 Maximum RGB values	14
4.5.4 Regularization	14
5.RESULTS	16
5.1 Approximate offset.....	16
5.2 Contralateral correspondence area coverage	17
5.3 Maximum RGB values	18
5.3.1 Results for the plantar feet.....	19
5.3.2 Results for the dorsal feet.....	21
5.3.3 Examinations without light	22
5.4 Regularization.....	23
6.DISCUSSION	24
6.1 Approximate offset.....	24
6.2 Contralateral correspondence area coverage	25
6.3 Maximum RGB values	26
6.4 Regularization.....	27
7.CONCLUSION.....	28
REFERENCES	29

LIST OF FIGURES

Figure 1.	The diagram in which the steps of the infrared thermography software are presented	8
Figure 2.	The segmented dorsal feet (green) and corresponding areas (yellow) illustrated	11
Figure 3.	Illustrations of the corresponding areas with default thermal_visual_approx_offset value (left) compared to thermal_visual_approx_offset value of 36 pixels (right).....	16
Figure 4.	The inner software mask displayed in the outcome of step 1 when the thermal_visual_approx_offset is 19 pixels (left) and 36 pixels (right).....	17
Figure 5.	The outcomes in which the contralateral temperature differences are displayed (left) and the filter is produced (right).....	18
Figure 6.	The inner software mask displayed in the outcome of the step 1 with different lighting settings.....	18
Figure 7.	The outcomes in which the segmented feet (green) and corresponding areas (yellow) are calculated for plantar side in varying lighting settings.....	19
Figure 8.	The outcome in which the temperatures of thermal image is mapped on the correspondence areas of both feet in visual image.....	20
Figure 9.	The outcome filter which indicates the areas in which the temperature difference exceeds 2.2 °C for plantar feet.	20
Figure 10.	The outcomes in which the segmented feet (green) and corresponding areas (yellow) are calculated for dorsal side in varying lighting settings.....	21
Figure 11.	The outcome filter which indicates the areas in which the temperature difference exceeds 2.2 °C for dorsal feet.....	22
Figure 12.	The outcomes of final filters when the value of problem_mask_regularization_pixel is 5 pixels (below) and 1 pixel (above).....	23

ABBREVIATIONS AND SYMBOLS

DFU	Diabetic foot ulcer
PVD	Peripheral vascular disease
RGB	Red, Green, Blue color model
ROI	Region of interest

1. INTRODUCTION

Diabetes can be defined as a set of conditions that are caused by a disorder of glucose metabolism in which hyperglycemia occurs (Egan and Dinneen, 2018). Hyperglycemia stands for high blood glucose and it is caused by the inability of the body to use or produce insulin to lower blood sugar levels (Cowap and Parry, 2015). Due to insulin insufficiency, the condition requires self-monitoring of blood glucose to decrease the risk of complications in diabetes (Cowap and Parry, 2015; Egan and Dinneen, 2018).

Diabetes is considered one of the most significant health issues globally due to the rise in the prevalence of diabetes cases. In 2021 the number of adults living with diabetes was 537 million and the number is expected to increase to 783 million by the year 2045. It is estimated that 6.7 million adults between the age of 20-79 have died due to diabetes and its complications in 2021. (International Diabetes Federation, 2021)

One of the major complications of diabetes is diabetic foot ulceration in which the feet are affected by wounds (Cassidy et al., 2021). Diabetic foot ulcers (DFUs) pose a risk of lower limb amputations and overall, they are one of the major causes of extremity amputations (Soo et al., 2020). The development of DFUs can be predicted with contralateral temperature differences due to raised skin temperature by the inflammation in affected lower limb (Golledge et al., 2022). The occurrence of DFUs is preventable in most cases and with monitoring of contralateral temperature differences, the areas of concern can be identified from the lower limbs (Machin et al., 2017).

Due to the importance of the information provided by the temperature differences in diabetic feet, infrared thermography has advanced as a medical imaging method to identify and prevent DFUs. In this thesis, the focus will be on the automatic contralateral temperature calculations of the infrared thermography software.

The focus of this thesis will be on analyzing the foundations of the error codes produced by the infrared thermography software and optimizing the parameters of the software. In relation to the applications of infrared thermography, diabetes, and its complications are introduced. The thesis intends to provide insight into infrared thermography imaging and its algorithm while studying the optimal functioning of infrared thermography software.

2. DIABETES AND ITS COMPLICATIONS

Diabetic foot ulceration is a diabetes-related complication in which the feet are affected by wounds (Cassidy et al., 2021). These foot complications are caused by a combination of different factors including diabetic neuropathy, peripheral vascular disease (PVD), foot deformities, and trauma (Dama et al., 2023; Kokkinos, 2019). Due to sensory impairment and insufficient blood flow, the tissue damage on the foot has a possibility to enlarge and get infected. (Kokkinos, 2019) The infections of diabetic foot ulcers (DFUs) can pose a risk of amputation of the lower limb (Cassidy et al., 2021).

In order to understand the relevance of preventative thermal imaging of DFUs, a brief overview of diabetes and its chronic complications related to DFUs is presented.

Chronic complications refer to diabetes-related complications that may develop over time and these may include for example kidney damage, foot complications, and diabetic neuropathy (Cowap and Parry, 2015). For this study, the focus will be on diabetic neuropathy and peripheral vascular disease in relation to DFUs.

2.1 Types of diabetes

Diabetes is a set of conditions characterized by hyperglycemia due to insulin insufficiency of the body (Cowap and Parry, 2015). The condition can be classified into four major groups including type 1 diabetes, type 2 diabetes, gestational diabetes, and other specific types of diabetes. The division between types of diabetes is defined by the cause of insulin insufficiency. All of the types are characterized by partial or total insulin insufficiency. (Egan and Dinneen, 2018) As the insulin of the body is produced by the beta cells in the islets of Langerhans of the pancreas, the insufficiency may be caused by insulin resistance of the body or the dysfunction of the pancreatic beta cells (Cowap and Parry, 2015).

Type 1 diabetes is characterized by the destruction of pancreatic beta cells which produce insulin. The destruction of these cells is caused by the autoimmune mechanisms of the body and due to this, type 1 diabetes is considered an autoimmune disorder. The condition is usually diagnosed during childhood or adolescence and it is not related to lifestyle or diet. (Cowap and Parry, 2015)

Type 2 diabetes, on the other hand, is more common in adults and it is characterized by insulin resistance or dysfunction of beta cells (Cowap and Parry, 2015; Egan and Dinneen, 2018). Insulin resistance denotes that insulin is produced but the body cannot use it to lower blood glucose levels. The hyperglycemia of type 2 diabetes can be also caused by the insufficient production of insulin due to pancreatic dysfunction (Cowap and Parry, 2015). There are several contributing risk factors associated with type 2 diabetes but some of the factors can be influenced by lifestyle choices. Due to this, the symptoms of this type of diabetes can be managed with healthy lifestyle choices. (Cowap and Parry, 2015)

Gestational diabetes is often a temporary condition in which insulin resistance arises during the late stage of pregnancy. Even though gestational diabetes may not include symptoms, high blood glucose levels may influence the developing baby. (Cowap and Parry, 2015) In other specific types of diabetes, the disease process is associated with factors that may include for example certain drugs, hormone excesses, mutations, or pancreatic disease (Egan and Dinneen, 2018). For example, insulin resistance may be caused by the excess of thyroid hormone which is associated with hyperthyroidism in which the production of the hormone in the thyroid gland is excessive (Cowap and Parry, 2015).

2.2 Diabetic neuropathy

Diabetic peripheral neuropathy refers to a diabetes-related condition in which the symptoms include dysfunction in peripheral nerves (Kokkinos, 2019). Hyperglycemia, characteristic of diabetes, causes damage to blood vessels and protective coverings of nerves causing difficulty in transmitting signals inside the body (Cowap and Parry, 2015). In diabetic neuropathy, both the sensory and motor nerves are affected in the lower limbs of the body. Frequently peripheral autonomic neuropathy is also prevalent leading to difficulties in thermoregulation of the lower limbs and a decrease in sweat secretion. (Lavery et al., 2010)

By impacting the sensory and motor nerves of the lower limbs, diabetic neuropathy can affect mobility. Due to possible sensory impairment, and difficulties in muscle coordination and strength, diabetic neuropathy can contribute to an increase in plantar pressure which is a factor contributing to diabetic foot ulceration. The loss of sensory functioning also poses a risk of tissue damage in the affected area. (Lavery et al., 2010)

2.3 Peripheral vascular disease

PVD is a condition of circulation in which the lower extremities of the body are affected by the atherosclerotic narrowing of blood vessels. In this condition, the metabolic requirements of the tissues are not met due to decreased blood perfusion in the lower extremities. The lack of perfusion causes a decrease in foot temperature. (Kokkinos, 2019)

Though being one of the major contributing factors in diabetic foot ulceration, PVD is not usually the only cause of ulceration. The tissue breakdowns are commonly caused by the combination of PVD and minor trauma. Due to insufficient blood flow to the area of injury, the possibility of ischemic ulceration and amputation rises. (Boulton, 1996) Insufficient blood flow induces the risk of ischemia of peripheral blood vessels which is a contributing factor in diabetic foot ulcers (Dama et al., 2023).

3. INFRARED THERMOGRAPHY IN DIABETIC FOOT ULCERATION

Infrared thermography is a method of imaging in which thermal energy is utilized to form infrared images in which the surface temperature distribution of the object of interest is visualized. Due to the thermal information provided, infrared thermography has been found to be a useful imaging tool for different purposes across multiple different application fields. (Meola, 2012) This thesis provides an overview of infrared thermography in relation to the thermal imaging of the DFUs.

3.1 Overview of infrared thermography

Thermal energy in the form of infrared radiation is emitted by all objects with a temperature above absolute zero. Infrared radiation is a form of electromagnetic radiation that is caused by the vibration of electrons. The thermal energy emitted is inversely proportional to the wavelength of the radiation and depends on the emissivity of the object. Emissivity is defined as the ability of energy emission of a surface. (Meola, 2012) Related to emissivity, the term blackbody is used for a surface in which all the radiation is absorbed and the emitted radiation radiates in a continuous spectrum (Bagavathiappan et al., 2013).

In infrared thermography, the information provided by infrared radiation is utilized to produce thermal images. The crucial part of the infrared thermography system is a detector that absorbs infrared radiation and creates an electrical signal based on the emitted energy. (Meola, 2012) The signals of the thermal data are processed with an image processing system (Ring, 2010). As infrared radiation is related to the surface temperature of the object of interest, thermal images provide information about the surface temperature distribution of the object of interest. (Meola, 2012)

As an imaging method, infrared thermography is a non-contact and non-invasive method which is an appropriate tool for repeated use due to the method not using any harmful radiation to produce information. Due to the provided temperature information and other advantages, infrared thermography is used for several purposes in different fields. Infrared thermography has been utilized for example in maintenance and pro-

cess monitoring, building inspections, non-destructive testing, and medicine. (Usamentiaga et al., 2014)

In maintenance infrared thermography has been found to be a useful tool to assess early signs of malfunctions as the abnormal temperature patterns as the imaging method can be utilized to identify faults in electrical connections or friction between materials. Additionally, in relation to insulation, infrared thermography can also produce for example visualization of possible energy losses in buildings. (Usamentiaga et al., 2014)

3.2 Medical infrared thermography

Thermoregulation of the human body is a vital ability in adjusting to a variety of environmental conditions. Sweating and modifications in circulation including the constriction and dilation of the blood vessels play a big role in controlling the surface temperature of the human body. (Ring, 2010) The overall temperature of the body surface is influenced by both environmental factors and the heat from the functions of the body including circulation and functions of the organs (Ring et al., 2015).

The surface of the body emits infrared radiation which can be used in medical thermal imaging to produce information about temperature distribution in the chosen area. This remote temperature sensing can be used to assess for example tissue viability and peripheral perfusion in blood vessels. (Ring, 2010) The human skin can be illustrated as a blackbody radiator due to its emissivity (Hardy and Muschenheim, 1934; Lahiri et al., 2012; Ring and Ammer, 2012).

The use of infrared thermography in the medical field started in the early 1960s even though the diagnostic relevance of infrared thermography in temperature measurement was recognized earlier (Lahiri et al., 2012; Ring et al., 2015). Infrared thermography has been used in research to study disease processes and due to the advances in imaging technologies, the studies have indicated that the imaging method can be utilized in diagnosis of multiple conditions including breast cancer and diabetic neuropathy (Lahiri et al., 2012).

In comparison with other medical imaging methods, infrared thermography provides a remote, non-invasive, and non-contact method of imaging. Due to the capturing of the natural radiation of the object of interest, the method doesn't expose to harmful radiation. However, infrared thermography may not be specific due to the influence of different factors on the surface temperature of the human body. (Lahiri et al., 2012)

In medical infrared thermography, the production of an electrical signal is conducted from the infrared radiation acquired from the human body (Meola, 2012). The regions of interest (ROI) are selected, and the signals of the thermal data are processed by image processing software. The use of masks in infrared thermography can be utilized to standardize images. The mask forms an outline for the anatomical structure in which the parts of the body are positioned (Ring, 2010)

3.3 Diabetic ulcer imaging

Due to the relation between blood perfusion and the surface temperature of the skin, infrared thermography can provide information about the physiological processes of the human body (Meola, 2012). As the temperature is affected by circulation, the method can be used to assess metabolism and circulation in diabetes (Ring, 2010). The changes in emitted energy of the skin surface will be shown in the infrared images.

The factors often prevalent in diabetic foot ulceration can be recognized with infrared thermography. The tissue breakdowns caused by trauma can be seen in infrared images as the wound changes the emissivity of the skin surface (Meola, 2012). The tissue viability and the effect of treatment in diabetic foot ulceration can be assessed with the monitoring of infrared thermography. (Ring, 2010)

As the prevention of DFUs requires self-care and monitoring of lower extremities to lower the risk of amputations and prevent DFUs, infrared thermography has proved to be an effective tool in preventing diabetic foot ulceration. Due to the identification of early warning signs, the prevention of DFUs is more effective with the modification of activities and protection of the affected lower limb. (Lavery et al., 2007)

The temperature difference of 2.2 °C as a limit has been studied in relation to diabetic foot ulceration to assess the contralateral temperature differences (Lavery et al., 2007). However, the temperature difference over the limit is not valid as a single measurement to predict ulceration due to the occasional occurrence of these temperature differences even without any foot complications. The results of the study indicated that the temperature difference that exceeds 2.2 °C should be detected in the same area during two consecutive days. (Wijlens et al., 2017)

4. METHODS

The study focuses on assessing the algorithms of the medical infrared thermography software by analyzing the foundations of error codes and optimizing parameters. The assessment of the algorithms is conducted with a created test environment in which the outcome of each step is displayed as an image. The patient data is retrieved from the database and processed in the infrared thermography software. The process utilizes parameter values that can be initialized before every run in the test environment. The modification of these values in relation to the outcome of the data processing in the infrared thermography software is analyzed.

4.1 Overview

The image processing of the infrared thermography software includes several steps in which the final outcome is produced (Figure 1). The software utilizes both thermal and visual images to calculate contralateral temperature differences of lower limbs.

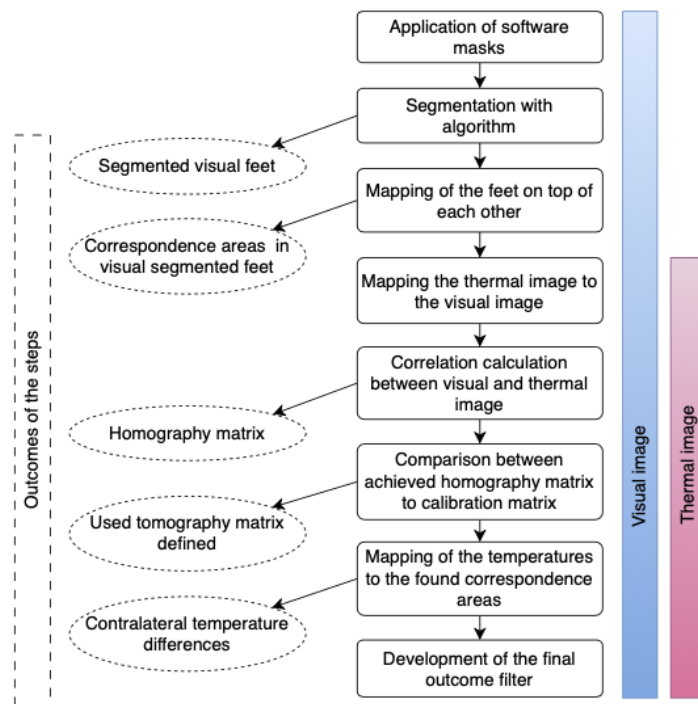


Figure 1. The diagram in which the steps of the infrared thermography software are presented

The process can be roughly divided into three sections which are image segmentation, symmetry and correspondence calculations, and temperature difference calculations. Visual images are utilized during the entire process, but the thermal image is used after successfully conducting segmentation and correspondence mapping. Before the process starts, the image to be processed through the system is assessed with the assistance of a parameter that defines the limit for the brightest pixel in the visual image and through this, excludes too dark images from the image processing.

The segmentation section includes the application of the software mask that assists in segmentation and the process of segmentation. Symmetry and correspondence calculations include both the mapping of the correspondence areas between visual feet and the mapping of the thermal image into the visual image. The assessment of the correlation between thermal and visual images is also included in this step. The final step consists of calculating the contralateral temperature differences and producing a visual representation of the results in which the temperature differences over 2.2 °C are indicated. Due to the validity of the result as a single measurement, the temperature differences over 2.2 °C detected in the same area during two consecutive days is utilized in the system but the focus of the analysis will be on the calculations of temperature differences.

4.2 Image segmentation

The segmentation of the foot from the background is conducted with visual images utilizing segmentation algorithms. It is conducted with visual images to achieve a high performance of the segmentation algorithm. Due to the usage of visual images, the probability of segmenting the whole area of interest is increased compared to the thermal images in which the lower temperatures may cause parts of the area to be cut off. The visual image segmentation also utilizes 3 channels, red, green, and blue color channels in RGB (red, green, blue) images to achieve more accurate results in segmentation.

The performance of image capturing is increased using masks. The software masks outline the area of interest to improve the standardization between images by assisting with the positioning of lower limbs (Ring, 2010). The infrared thermography software in this study utilizes two separate masks that outline the shape of the foot. The outer mask limits the area in which the segmentation occurs, and the aim of the inner mask is to be covered by the segmented object and it also provides information about the texture of the object of interest.

The segmentation method in which the object of interest is extracted from the background is utilized. The method uses a rectangle shape which is placed around the desired object. (Brahmbhatt, 2013) The segmentation uses both texture and edge information to extract the object from the background. The texture information refers to the color of the image and the edge information to the contrast of the image. (Rother et al., 2004)

The segmentation aims to extract the lower limbs from the background and due to this, the success of this step is defined by the precision of the segmentation. In successful segmentation, the entire area of the foot is extracted from the image without extracting any background along the edges of the segmented foot. The segmentation finds both lower limbs and their outlines are successfully defined. The infrared thermography software also assesses the possible size difference between lower limbs through a parameter value and limits the processing of images in which the size difference is notable.

4.3 Symmetry and correspondence calculations

The step of symmetry and correspondence calculations consists of two main steps and the assessment of the successful execution of the steps. The main steps consist of calculations conducted between feet in visual images and the calculations between thermal and visual feet. The introduction of these main steps is presented.

The calculations between feet are conducted with the assistance of visual images and the software masks are utilized to form the correspondence between feet. Both thermal and visual images are utilized in calculations between thermal and visual feet. Thermal coordinates are utilized in conducting all the calculations.

4.3.1 Calculations between feet in visual images

The symmetry calculations are conducted to acquire information about the contralateral correspondence of the feet. The contralateral correspondence is mapped by mapping the segmented feet of the visual image on top of each other. The association between contralateral areas is created through the mapping to achieve symmetry between lower limbs. The comparison between contralateral areas is conducted with the assistance of the software masks used in infrared imaging. In this section of the process, the correspondence areas of lower limbs are acquired only with visual images.

The success of the algorithms in finding the correspondence areas is assessed with a parameter value that indicates the percentage of the correspondence area coverage in the segmented foot. The default value defines the limit which is needed to be achieved to proceed in image processing without an error code. In successful correspondence calculations, the correspondence areas cover most of the area in segmented feet (Figure 2).

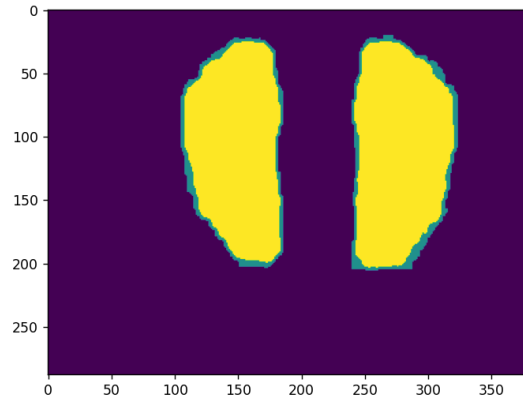


Figure 2. *The segmented dorsal feet (green) and corresponding areas (yellow) illustrated*

The segmented feet are illustrated as green areas and found correspondence is displayed with yellow areas. As the figure illustrates, the green area is mostly covered by the yellow area which indicates that the correspondence is found symmetrically from the segmented feet.

4.3.2 Calculations between thermal and visual feet

In this study, the camera used in infrared thermography includes two lenses in which the other one takes the thermal image and another one the visual image. To achieve accurate symmetry calculations, the camera must be calibrated by formulating a calibration matrix that takes into account the alignment and distance between two lenses. This distance between images is 24 pixels in the cameras used in this study when the imaging is conducted at the typical imaging distance of 52 cm. The alignment between lenses is compensated mathematically by calculating a homography matrix for each camera. The information achieved through calibration is fetched by the image processing algorithms according to the serial number of the used camera.

After the symmetry between feet in the visual images is achieved, the thermal image is mapped to the visual images with the homography matrix created in calibration. The correlation between the feet in the thermal images and the symmetric segmented foot in the visual images is calculated. The correlation must exceed a certain limit defined

by a default parameter value to be able to map the correspondence between visual and thermal foot. The parameter defines whether the correlation calculations are successful. Due to the possible coldness of the foot, the correlation may not exceed the limit but when the limit is passed, a new homography matrix between thermal and visual images is created. This represents the calculated mathematical compensation of the different alignments and distance between two lenses of the thermal camera. The newly created homography matrix aims to increase the accuracy of the homography matrix calculated in calibration but the new matrix is also compared to the original matrix as the new homography matrix may not differ considerably from the calibration.

4.4 Temperature differences

Temperatures for the segmented feet from visual images can be calculated as the correlation of the segmented feet and corresponding areas in the thermal image are known. The resolution of the thermal image is lower than in the visual images and due to this, one pixel in the thermal image is divided into multiple pixels in the visual image. The comparison between temperatures is conducted with the set of pixels located in the footprint of the larger foot. Due to the selected set of pixels from the larger foot, the mapping of the pixels on top of the smaller foot may not be exact.

The algorithm in the infrared thermography software calculates the temperatures for the segmented feet from visual images by mapping the temperature values from the thermal image to the area where the correspondence is found. The area of correspondence is an area in which the larger foot's corresponding points are mapped on the area of the smaller foot. The common set of points is used to compare the contralateral temperatures.

The contralateral temperature differences are utilized to produce a filter that indicates the areas in which the temperature difference is over 2.2 °C. The areas of interest are mapped in the common set of points in which the temperatures of both feet are mapped. Due to this, the areas of interest are mirrored on top of the larger foot from the common set of points on top of the smaller foot. As a result of the algorithms in the infrared thermography software, the created filter is mapped on top of the original thermal image to indicate the contralateral temperature differences.

4.5 Inspection of the parameters

This thesis focuses on analyzing the foundations of the error codes and due to the incidences of different error codes, the appropriate parameters associated with the most

frequent error codes were assessed. The parameters assessed are associated with the steps of image processing in infrared thermography software. The analysis was conducted in the created test environment.

The functioning of the studied parameters is introduced to provide background information about the operations of the infrared thermography software in relation to the parameters. Due to the scope of the thesis, the study focuses on assessing four parameters which are associated to frequent error codes.

4.5.1 Approximate offset

The approximate offset is defined as the pixel distance between thermal and visual images caused by the distance between thermal and visual lenses. This pixel distance is initialized with the parameter *thermal_visual_approx_offset*. The default value of the parameter is 24 pixels with a typical imaging distance of 52 cm. The value of the parameter affects the positioning of the software mask used in correspondence calculations.

The value of the parameter *thermal_visual_approx_offset* was analyzed through images of lower limbs in which the infrared thermography software produced an error code after symmetry calculations for a plantar image. The error code occurred after the contralateral areas were identified. The test image was processed in the test environment by initializing the parameter *thermal_visual_approx_offset* with values between 19 and 36 pixels to examine the functioning of the algorithms. The values were chosen according to the correct positioning of inner software masks in which the masks are covered by the lower limbs.

4.5.2 Contralateral correspondence area coverage

After the contralateral correspondence of the lower limbs is calculated, the infrared thermography software inspects the positioning of the correspondence area in the smaller foot. The parameter *common_mask_covers_at_least* defines what is the percentage of the area in the segmented foot covered by the correspondence area in which the image is accepted without an error code.

The default value for *common_mask_covers_at_least* is 80%. The effect on parameter value was tested with an image in which the outcome indicated that the correspondence areas do not accurately cover both feet. With the default value, the system produced an error code. The parameter value of *common_mask_covers_at_least* was

tested by initializing the value to 50% to analyze the functioning of the infrared thermography software in the case of asymmetrical correspondence areas.

4.5.3 Maximum RGB values

The darkness of the image is examined in the infrared thermography software through the parameter *too_dark_image_max_value*. The value of this parameter limits the value of the brightest pixel in the visual image and produces an error code when the brightest pixel is below the initiated parameter value. Visual images include three RGB components and the maximum values of each channel are compared to find the overall maximum value.

The parameter of *too_dark_image_max_value* was examined separately for the plantar and dorsal feet. The parameter was assessed with 3 levels of lighting for the dorsal and plantar sides of the lower limbs and with an entirely black image. The default value of the parameter was used which is the value of 30. The value indicates that the maximum RGB value found from the image must be under 30 for the system to produce an error code about the darkness of the visual images.

For the feet in dorsal and plantar images, the infrared thermography software produced a good segmentation of the feet and appropriate correspondence calculations in the brightest test lighting and these results are compared with the test images with lower lighting. Due to the functioning of the parameter *too_dark_image_max_value* with the maximum RGB value of the image, the test environment was programmed to display the calculated maximum RGB value for each visual image for plantar and dorsal feet.

The infrared thermography software was also tested with an entirely black image to examine the functioning of the system with the default parameter value of *too_dark_image_max_value*. For these tests, the calculated maximum RGB value was displayed for the entire black images. Due to the results, further studies were conducted in a dark room with visual lens covered with a black surface. These studies were conducted with the default value of 30. The parameter value was also initialized to 90 to test whether the system limits the images with too low levels of lighting.

4.5.4 Regularization

In infrared thermography software, the final filter produced on top of the thermal image is regularized by a specific number of pixels. These pixels of regularization are initialized with the parameter *problem_mask_regularization_pixels*. The default value of the

parameter is 5 pixels, and it was assessed by adjusting the value to 1 pixel in which the system does not execute any regularization on the final filter.

With the default value of 5 pixels, the filter is regularized by the values of the area of 5 pixels. Without any regularization, the values of each pixel are portrayed according to the temperature difference found in each pixel. The examination of the parameter was conducted on the set of plantar images which were used to assess the darkness of the images due to the difference in the final filters. The test aimed to assess the effect of regularization on the final filters produced during image processing.

5. RESULTS

In this study, the test environment was created to analyze the parameter values of the medical infrared thermography software. The effect of the initialized parameters on the algorithmic calculations of the software was evaluated by analyzing the outcomes of each step. The testing included test images of the lower limbs and the outcomes of the steps display images in pixel coordinates.

5.1 Approximate offset

The parameter *thermal_visual_approx_offset* was analyzed with images of lower limbs in which the error code was produced. With the default value of the parameter, the correspondence mapping between contralateral areas caused an error code. The outcome of the step prior to the error code was an image in which the correspondence areas displayed in yellow do not symmetrically match and the area of the other foot does not cover the segmented area displayed in green. When the test image was processed in the test environment, the infrared thermography software proceeded without an error code with a test value of 36 pixels. The outcome of the correspondence calculations with the value of 36 pixels was compared with the outcome of the default value of the parameter *thermal_visual_approx_offset* (Figure 3).

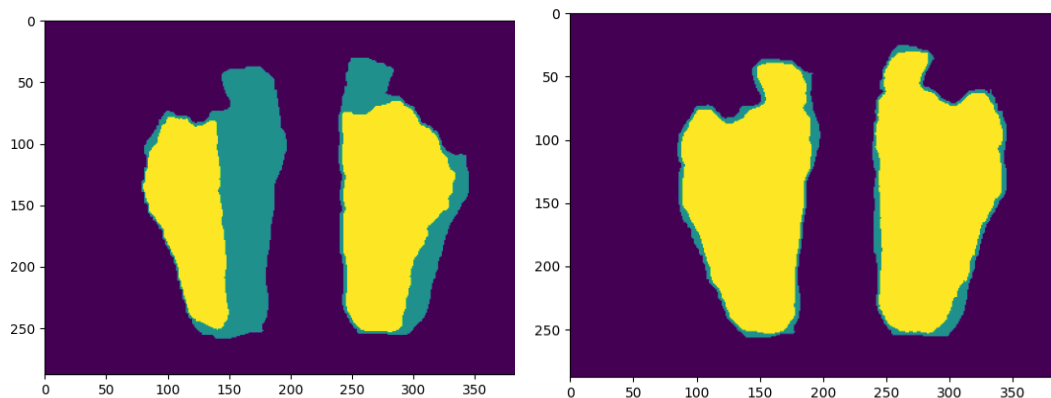


Figure 3. Illustrations of the corresponding areas with default *thermal_visual_approx_offset* value (left) compared to *thermal_visual_approx_offset* value of 36 pixels (right).

With the *thermal_visual_approx_offset* value of 36 pixels, the algorithms proceeded without an error code and through the correspondence, the contralateral temperature differences were able to be accurately calculated. As the parameter affects the correspondence calculations through the position of the software masks, the step in which the positioning of the masks is displayed was also assessed (Figure 4).

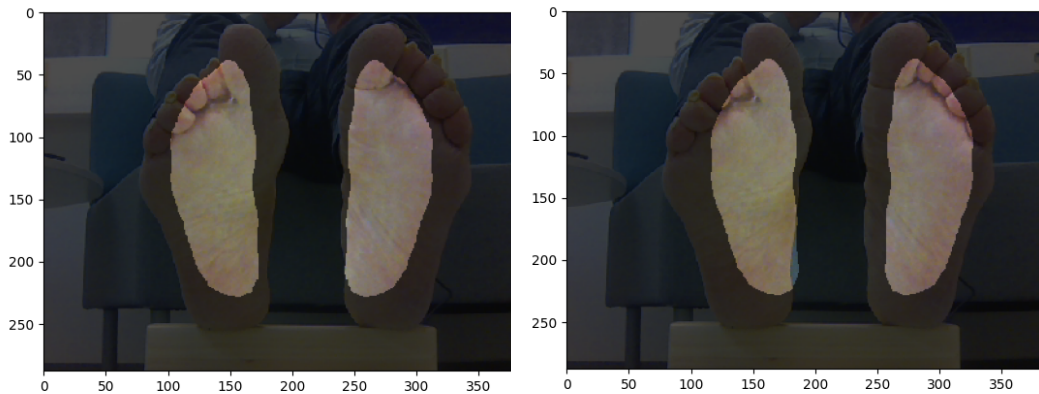


Figure 4. The inner software mask displayed in the outcome of step 1 when the *thermal_visual_approx_offset* is 19 pixels (left) and 36 pixels (right).

The outcome of the step includes an image in which the inner software mask is displayed on the visual image. Through analyzing the images of this step, it is apparent that with lower values of *thermal_visual_approx_offset*, the inner software mask is positioned more to the left side of the image, and initializing with higher values, the mask is moved more to the right.

The results illustrated that when the parameter value is modified to position the inner software mask accurately, the correspondence can be calculated without an error code. With the value of 36 pixels, the environment created an outcome in which the correspondence can be accurately calculated.

5.2 Contralateral correspondence area coverage

The parameter *common_mask_covers_at_least* was assessed with a test image in which the error code was produced with the default parameter value due to the differences between correspondence areas of the feet (Figure 3). The value of the parameter was modified to 50% in which the infrared thermography software conducted the contralateral temperature difference calculations without an error code. The system found a contralateral temperature difference based on the comparison of the contralateral temperatures (Figure 5).

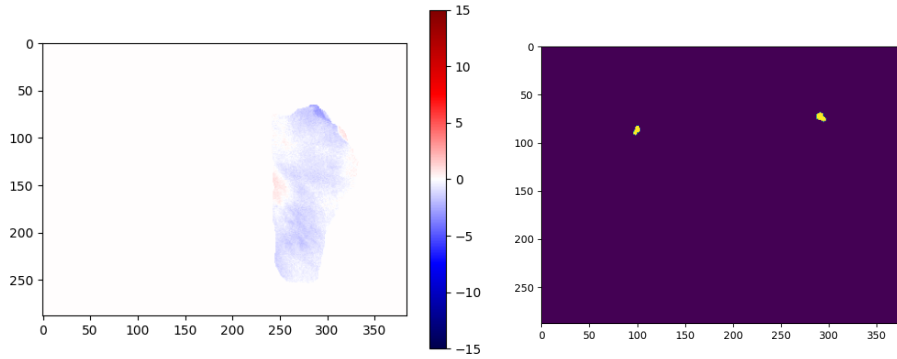


Figure 5. The outcomes in which the contralateral temperature differences are displayed (left) and the filter is produced (right).

Despite the inaccurate correspondence areas in the feet, the infrared thermography software produced a suitable image in which the difference in contralateral temperatures is indicated with either blue or red. In the image, the temperatures are compared between correspondence areas, and the greater temperature differences are indicated with the stronger color in either color. The system found one area in which the contralateral temperature difference exceeds the limit of $2.2\text{ }^{\circ}\text{C}$ and it is indicated in the produced filter.

5.3 Maximum RGB values

The parameter value of *too_dark_image_max_value* was assessed with 3 levels of lighting. The difference in lighting between test images is illustrated in the first outcome of the image processing (Figure 6). As the parameter was assessed separately for the plantar and dorsal feet, the results are presented separately.

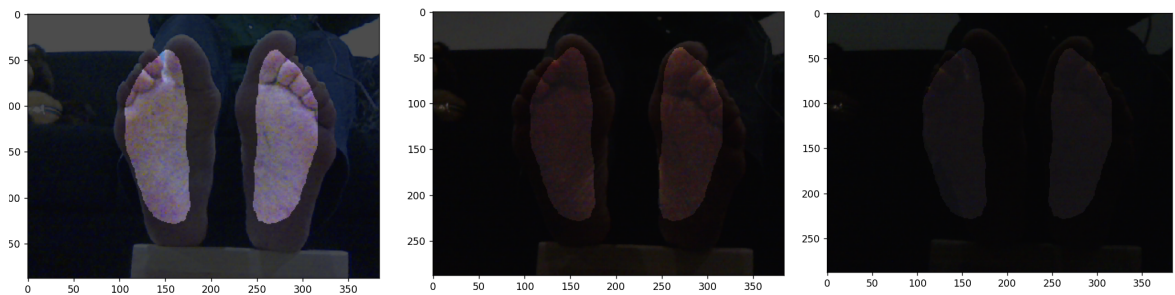


Figure 6. The inner software mask displayed in the outcome of the step 1 with different lighting settings.

Further studies conducted with entirely black images were also included in the assessment of the parameter *too_dark_image_max_value*. The results are presented after the results for the plantar and dorsal images. For all the images, the test environment displayed the maximum RGB value of each image.

5.3.1 Results for the plantar feet

The infrared thermography software produced the calculated maximum RGB value for each visual image for plantar feet (Table 1) As the results illustrate, the maximum values remain considerably high despite the lighting of the image. The values express a decrease when the level of lighting is decreased but the differences between the values of test images is not considerable.

Table 1. The calculated maximum RGB value for each test lighting environments for the plantar feet

The lighting of the plantar image	Maximum RGB value of plantar image
Maximum	255
Medium	254
Minimum	230

Due to the acquired maximum RGB values, none of the test images is rejected as too dark and the image processing is conducted for each image. The correspondence calculations are conducted to all test images. The system produced outcomes in which the effect of lighting is illustrated in segmentation and correspondence calculations (Figure 7).

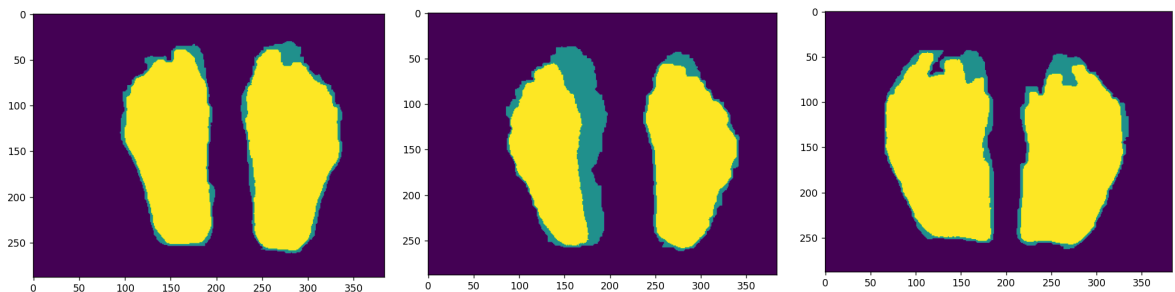


Figure 7. The outcomes in which the segmented feet (green) and corresponding areas (yellow) are calculated for plantar side in varying lighting settings.

The outcome of the maximum lighting is presented on the left, and the outcome of the medium lighting in the middle and on the right side is the result of minimum lighting. The segmented area, illustrated with green color, indicates how the segmentation result is affected by the lighting. For the plantar side, the shape remains consistent with maximum and medium lighting, but the shape is distorted when the segmentation is conducted with minimal lighting.

As the correspondence calculations depend on the segmentation step, the found correspondence area is smaller in the distorted feet when the segmented area is also

smaller on the dorsal side. Even though the segmentation of the plantar feet in medium lighting does not indicate distortion, the found correspondence is not symmetrical between lower limbs. The minimum lighting image for the plantar side finds the correspondence of the feet but the correspondence areas include points from the background of the lower limbs. This is due to the segmentation proceeding further in the visual images including some background in the segmented feet due to the level of lightness affecting the functioning of the segmentation algorithm.

The outcome of mapping the temperatures of the thermal image to the correspondence areas of visual images illustrates how the segmentation of plantar feet in minimal lighting includes a background in the correspondence areas in which contralateral temperature is calculated (Figure 8). The darker green indicates the lower temperature values from the background of the lower limbs.

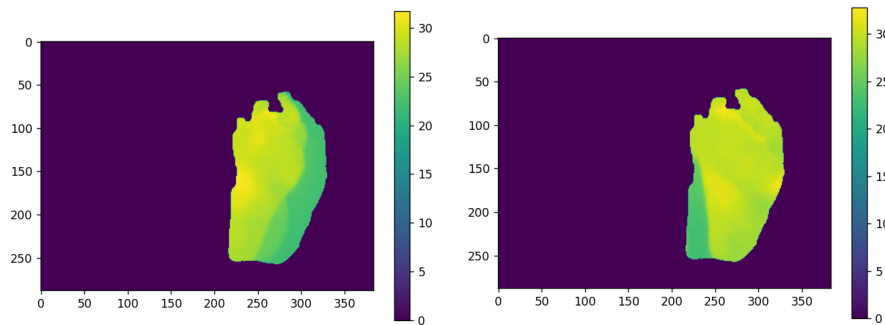


Figure 8. The outcome in which the temperatures of thermal image is mapped on the correspondence areas of both feet in visual image.

The distortions during the segmentation and symmetry calculations affected the final filter produced in which the contralateral temperature differences are indicated. For the plantar side, the outcomes of the infrared thermography software indicated that the areas, in which the contralateral temperature differences are detected, increase when the lighting is decreased from the maximum to minimum lighting (Figure 9).

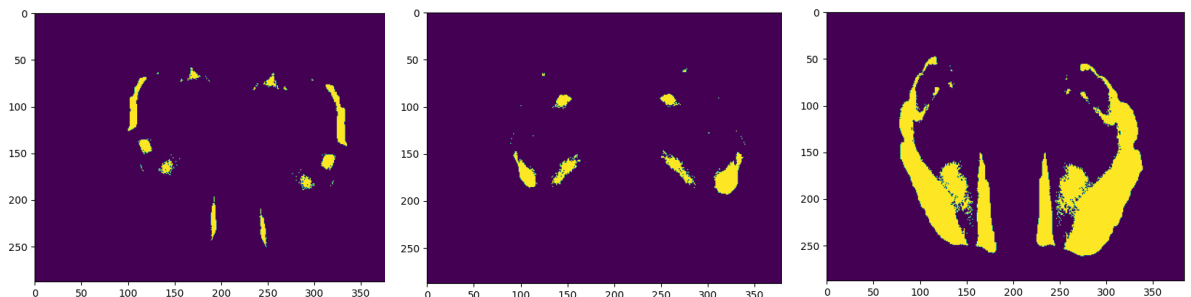


Figure 9. The outcome filter which indicates the areas in which the temperature difference exceeds 2.2 °C for plantar feet.

The level of lighting affects the calculations of contralateral temperature differences. Due to the distortions in the segmentation and correspondence calculations, the system produced different filters in which the contralateral temperature differences are indicated for plantar images.

5.3.2 Results for the dorsal feet

The different lighting levels were also used to assess the dorsal images. The infrared thermography software calculated the maximum RGB value for the dorsal images of the lower limbs (Table 2). Compared to the plantar values (Table 1), the dorsal values also decrease when the lighting decreases. The decrease between images is more notable for the dorsal images.

Table 2. The calculated maximum RGB value for each test lighting environments for the dorsal feet

The lighting of the dorsal image	Maximum RGB value of dorsal image
Maximum	230
Medium	172
Minimum	111

The results indicate that the values exceed the limit value in every tested lighting and the images are processed. The infrared thermography software produced outcomes in which the results of segmentation and correspondence calculations are illustrated. In these results, the effect of the difference in lighting is visible (Figure 10). For the dorsal feet, the area of segmented feet decreases with the decreasing light and the shape of the feet becomes more distorted. The correspondence areas remained symmetrical and inside the feet due to decreasing area of segmented feet.

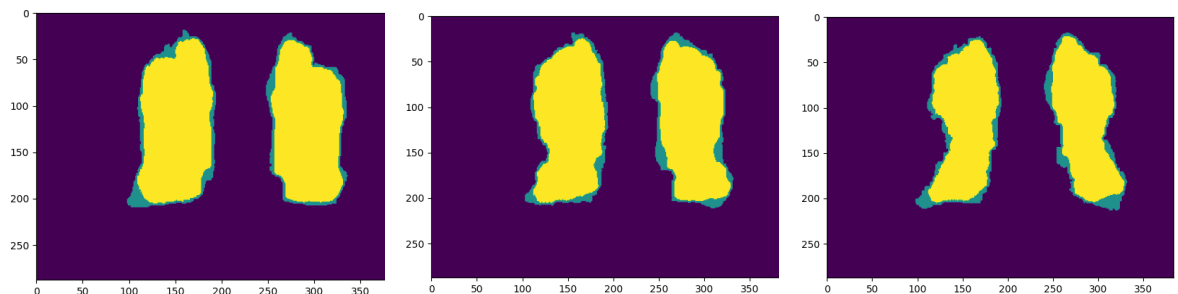


Figure 10. The outcomes in which the segmented feet (green) and corresponding areas (yellow) are calculated for dorsal side in varying lighting settings.

The infrared thermography software produces the outcome filters according to the previous steps conducted in the process. For the dorsal side, the outcomes indicate that

the areas in which the temperature difference is found decrease when the level of lighting decreases (Figure 11). This is due to the smaller area extracted through segmentation.

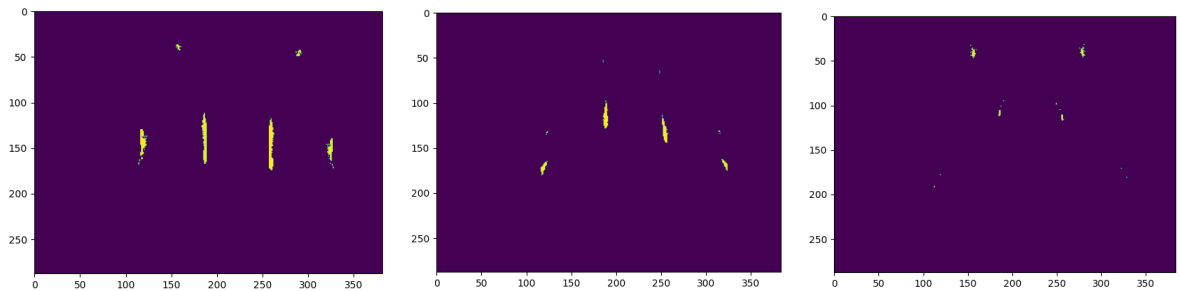


Figure 11. The outcome filter which indicates the areas in which the temperature difference exceeds 2.2 °C for dorsal feet.

The shapes of the filters are influenced by the results of segmentation and symmetry calculations. Even though the symmetry calculations find symmetrical corresponding areas, the areas are found in the segmented feet. The result of segmentation becomes narrower when the lighting decreases and due to this, parts of the feet are cut off during segmentation. These areas are left out of the correspondence calculations.

5.3.3 Examinations without light

The parameter *too_dark_image_max_value* was assessed with entirely black images. When processing the image, the log file of the run indicated that the system tried to create a segmentation mask for the image, but the mask scaled back to the original size. The system also utilizes a parameter *min_mid_mask_covering_fraction* before the error code “*Feet do not cover the inner templates*” is produced.

Further studies in a dark room showed that the lowest value of the maximum RGB value of a visual image was 37. Compared to the default value of 30, which was aimed to prevent the use of too dark images, the found value remained higher. Due to this, the images were not rejected as too dark.

When the parameter value was changed to 90, the infrared thermography software produced an error code of “*Too dark image*”. The error code indicates that the system examines whether the maximum RGB value is under the value of the parameter *too_dark_image_max_value*.

5.4 Regularization

The infrared thermography software produced outcomes in which the effect of the parameter *problem_mask_regularization_pixels* is visible in the plantar filters (Figure 12). With the test value of 1 pixel, the system produces filters represented in the first row and the second row illustrated the same filters with the parameter value of 5 pixels.

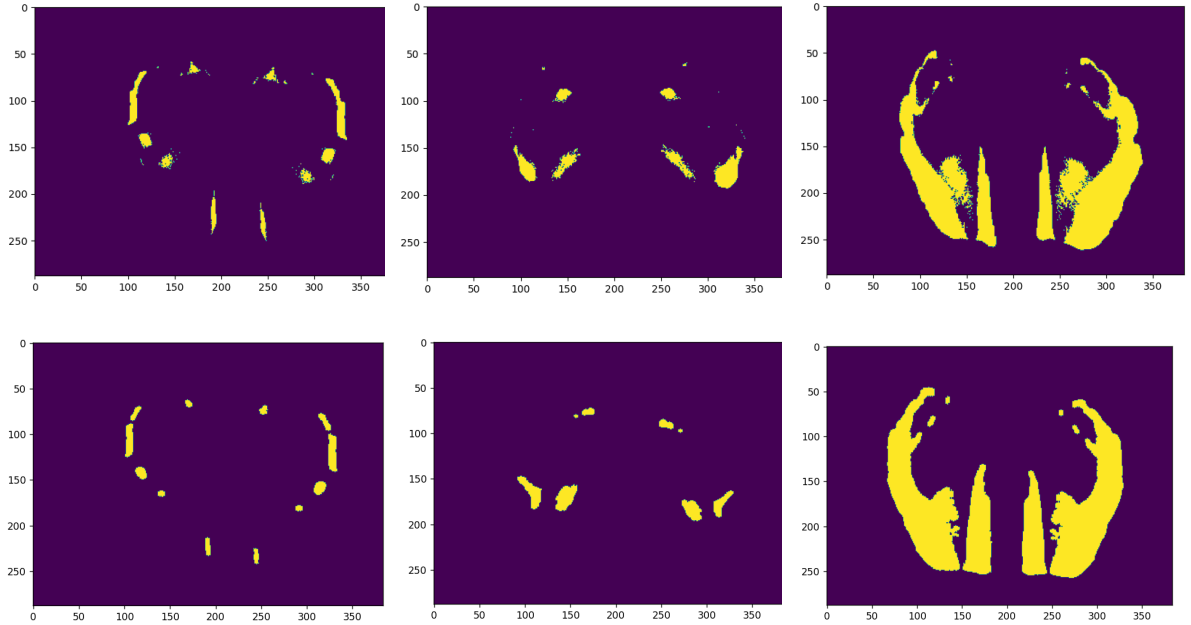


Figure 12. The outcomes of final filters when the value of *problem_mask_regularization_pixel* is 5 pixels (below) and 1 pixel (above).

The results illustrate that the individual pixels in which the temperature difference is detected are blocked out of the outcome filter with regularization. Due to this, the shapes of the produced filter include fewer individual pixel areas with the default value of the parameter. The regularization adjusts the borders of the shapes to be rounder and connects the different sets of points located closely. Due to this, the borders and shapes are more defined, but the individual points are limited out of the outcome. The shapes also increase in size due to the connection between different sets of pixels in which the contralateral temperature is detected.

6. DISCUSSION

The focus of the thesis was to analyze the foundations of the error codes and optimize parameters of infrared thermography software. Based on the results acquired from the test environment, the studied parameters can affect the results of image processing in infrared thermography software. Some of the studied parameters function as restrictions to limit the processing of images in which the requirements of quality are not achieved during the process. The other studied parameters affect how infrared thermography processes the images. The results are discussed more in detail individually for each parameter.

6.1 Approximate offset

The examination of the parameter *thermal_visual_approx_offset* illustrated that the parameter affects the positioning of the inner software mask during the first steps of the image processing through the horizontal positioning of the software masks. The correspondence calculations are dependent on the positioning of these masks since the comparison between feet in the visual images is conducted with the assistance of the inner software mask.

The results indicated that the inaccuracies produced during the image processing in the infrared thermography system can be corrected with the assistance of the parameter *thermal_visual_approx_offset*. The parameter is dependent on the imaging distance in which the imaging is conducted. Typical imaging distance is defined to be 52 cm but in different imaging situations, the distance may vary. The tests were conducted on plantar images due to the frequently occurring error code which was not produced for the dorsal images. This indicates that the default parameter value appears to be suitable for the dorsal images, but the plantar side seems to have more variety and the correspondence is not always calculated correctly.

The other factors in the imaging situation may also influence the final positioning of the software masks in the visual images. As the imaging can be conducted by the patient himself, the imaging environment and the patient may pose potential sources of errors in the imaging situation. Numerous factors including the mobility of the patient, and the size or positioning of the target lower limbs may result in inaccurate positioning of the

inner masks on top of the lower limbs in visual images. Due to these factors, the value of the parameter could be modifiable, if the modification is needed.

The infrared thermography software also examines whether the positioning of the correspondence area in the smaller foot is accurate with the parameter *common_mask_covers_at_least* and due to this, the system produces an error code if the system produces inaccurate correspondence calculations. This test indicates whether the value of the parameter *thermal_visual_approx_offset* is suitable for the used image. The parameter *common_mask_covers_at_least* could be used to assess the validity of the approximate offset value for each image.

6.2 Contralateral correspondence area coverage

The positioning of the correspondence area in the smaller foot is assessed with the parameter *common_mask_covers_at_least* and the results illustrated that the parameter defines the limit for the coverage percentage of the correspondence area on top of the segmented area of the smaller foot. Even though the lower values of the parameters produced seemingly accurate results in contralateral temperature calculations without producing an error code, due to the inaccuracies in the correspondence calculations, the final filter may not represent the real situation.

One area, in which the contralateral temperature difference passes over the limit of 2.2 °C, was detected during the test when the parameter value was 50 %. Due to the inaccurate correspondence calculations, the found contralateral temperature difference may not be accurate as the system may have compared temperatures between different areas of the feet. Due to the distortion, the validity of the results may not be sufficient to provide accurate information about the contralateral temperature differences if the value of the parameter *common_mask_covers_at_least* is too low even though the system does not produce an error code.

The results indicate that contralateral correspondence calculations can be conducted to low-quality correspondence images when the value of the parameter is initialized lower. In these cases, the error code is not produced, and the low-quality correspondence images pass the calculations. The parameter functions as a quality constraint to limit the number of calculations conducted on images in which the correspondence calculations produced nonsymmetric outcomes.

To prevent the rejection of images due to the parameter value, the correspondence area coverage should exceed the defined limit. As mentioned, when assessing the parameter value of *thermal_visual_approx_offset*, the images rejected by the parameter

value of *common_mask_covers_at_least* can be corrected with accurate approximate offset.

6.3 Maximum RGB values

The assessment of the parameter *too_dark_image_max_value* illustrated that the maximum RGB values received from the test images for both plantar and dorsal feet exceed the default limit of 30 in every tested lighting. Due to this, the test images were accepted without an error code for both plantar and dorsal feet. The examination with an entirely black image demonstrated that even the maximum RGB value of the black image resulted in a value of 37 which also exceeds the default limit.

The result of testing the black image with a parameter value of 90 illustrated that the error code is produced if the found maximum RGB value remains under the limit. Based on the result, the infrared thermography software examines whether the image is too dark but the found maximum RGB values of the test images exceed the limit. This indicates that the default value of *too_dark_image_max_value* is too low to limit the dark images.

The maximum RGB values of the plantar images remain considerably high even in the darkest lighting contrary to the dorsal values which decrease when the lighting is decreased. The difference in the values may be caused by reflections of light in background of dorsal images as the maximum value is received from the brightest pixel of the visual image.

With the presumption, that lower limbs will be positioned correctly to cover the inner software templates, the maximum RGB value could be fetched inside the inner software mask as it includes the object of interest. Regardless, the lower limbs are segmented from the background, and due to this, the maximum RGB values found in the background may not be relevant in image processing. The statistical method could be used to calculate the maximum RGB value to even out the individual maximum values caused by reflections or other possible light sources.

The results indicated also that the maximum RGB value remained around 37 even with black images. This may be caused by the possible disruption from the sensors of the camera or by the internal noise of the camera. With the maximum value of 37, the channels of the images remain still considerably dark which may also indicate that the imaging situation still included some sources of error. Overall, capturing a perfectly dark image may be impossible.

The exclusion of images with low lighting plays a crucial part in segmentation due to the distortions. For both the plantar and dorsal sides, the segmentation was affected, and the edges of the lower limbs were difficult to detect from the images by the algorithm. This resulted in the inclusion of the background of the image and narrowed shapes. As the segmentation influences the following steps of the image processing, the filter produced varies to some extent between different lighting for both dorsal and plantar images. Due to the distortion in segmentation and difference in filters, it appears that the quality of the contralateral temperature difference is affected by the lower-level lighting. The parameter *too_dark_image_max_value* plays an important role in image processing and the value could be studied more to find a suitable default value to limit images with too low levels lighting.

6.4 Regularization

The regularization of the outcome filter was studied with the assistance of the parameter *problem_mask_regularization_pixels*. The assessment of the default parameter value indicated that the regularization limits the individual pixels in which the contralateral temperature difference is detected. Due to this, the regularization limits the possible aberrations caused by the other stages of image processing. The individual pixels, in which the temperature difference is detected, may not provide relevant information about the contralateral temperature differences between lower limbs.

The filter with no regularization provides more information about the results of the calculations and smaller areas can be detected more precisely but the number of possible errors may increase. The regularization can be utilized to smooth out the errors that occurred during the previous steps of image processing. The lowering of the regularization may increase the possible errors and due to this, some regularization should be utilized during the automatic contralateral correspondence calculations. The probability of detecting a contralateral temperature difference in the same area may increase when the smaller pixel areas are not excluded from the images by regularization.

Due to these factors, the value of the parameter *problem_mask_regularization_pixels* could be modifiable to serve the different needs of image processing. To receive more information, the infrared software thermography software could also provide multiple outcomes which are produced with multiple different values of the parameter. Results of the assessment also illustrate that no regularizations represent most accurately the outcome of the contralateral temperature difference calculations and the overall functioning of the infrared thermography software. Due to this, the images with no regularization could possibly be utilized to assess the functioning of the algorithms.

7. CONCLUSION

The aim of the thesis was to analyze the foundations of the error codes and optimize the parameters of the infrared thermography software. The assessment included an inspection of a set of parameters associated with the image processing algorithms and the test was conducted in a created test environment.

The results indicated that image processing of the infrared thermography software is influenced by the studied parameters. The study revealed that the optimal functioning of the algorithms could be achieved by optimizing the parameters associated with specific steps of image processing. The study also identified complexities that need to be taken into consideration when finding the optimal values of the parameters.

Based on the findings of the study, the imaging situation or environment may include sources of error that may influence image processing. Due to this, the optimal parameter values of the infrared thermography software should be studied further to achieve suitable calculations and adaptive image processing.

Infrared thermography as a non-invasive method of medical imaging, in which the physiological information is acquired as a form of infrared radiation, is becoming a more accurate tool to assess abnormal temperature patterns of the human body. Due to this, the usage of infrared thermography in diagnostics may increase in the future.

Due to the increasing prevalence of diabetes, diabetic foot ulceration will most likely remain a relevant health issue also in the future. As there is evidence that the contralateral temperature differences can predict the development of DFUs, the contralateral temperature difference calculations embedded into infrared thermography can be used as a method to enhance the prevention of DFUs.

REFERENCES

- Bagavathiappan, S., Lahiri, B.B., Saravanan, T., Philip, J., & Jayakumar, T. (2013). Infrared thermography for condition monitoring – A review. *Infrared physics & technology* Volume 60, 35–55. Available at: <https://doi.org/10.1016/j.infrared.2013.03.006> (Accessed: 12.04.2023)
- Boulton, A. J., & Shaw, J. E. (1996). The Pathogenesis of Diabetic Foot Problems: an Overview. *Diabetic Medicine* 13, S12–S16. Available at: <https://doi.org/10.1002/dme.1996.13.s1.12> (Accessed: 07.02.2023)
- Brahmbhatt, S. (2013). *Practical OpenCV*, 1st ed. 2013. ed, Technology in action Practical OpenCV. Apress, Berkeley, CA. Available at: <https://doi.org/10.1007/978-1-4302-6080-6> (Accessed: 14.02.2023)
- Cassidy, B., Reeves, N.D., Pappachan, J.M., Gillespie, D., O’Shea, C., Rajbhandari, S., Maiya, A.G., Frank, E., Boulton, A.J., Armstrong, D.G., Najafi, B., Wu, J., Kochhar, R.S., & Yap, M.H. (2021). The DFUC 2020 Dataset: Analysis Towards Diabetic Foot Ulcer Detection. *European Endocrinology* 17, 5–11. Available at: <https://doi.org/10.17925/EE.2021.17.1.5> (Accessed: 07.02.2023)
- Cowap, N., & Parry, N.M. (2015). *Diabetes, MyModernHealth FAQs*. Mercury Learning and Information, Dulles, Virginia
- Dama, G., Du, J., Zhu, X., Liu, Y., & Lin, J. (2023). Bone marrow-derived mesenchymal stem cells: A promising therapeutic option for the treatment of diabetic foot ulcers. *Diabetes Research and Clinical Practice* 195, 110201. Available at: <https://doi.org/10.1016/j.diabres.2022.110201> (Accessed: 07.02.2023)
- Egan, A.M., & Dinneen, S.F. (2018). What is diabetes? *Medicine* 50 (10), 615-618. Available at: <https://doi.org/10.1016/j.mpmed.2018.10.002> (Accessed: 26.01.2023)
- Golledge, J., Fernando, M.E., Alahakoon, C., Lazzarini, P.A., aan de Stegge, W.B., Netten, J.J., & Bus, S.A. (2022). Efficacy of at home monitoring of foot temperature for risk reduction of diabetes-related foot ulcer: A meta-analysis. *Diabetes/metabolism research and reviews* 38, e3549-n/a. Available at: <https://doi.org/10.1002/dmrr.3549> (Accessed: 05.04.2023)
- Hardy, J.D., & Muschenheim, C., (1934). The radiation of heat from the human body. Iv. The emission, reflection, and transmission of infra-red radiation by the human skin. *The Journal of clinical investigation* 13 (5), 817–831.
- International Diabetes Federation, (2021). *IDF Diabetes Atlas | 10th edition*. International Diabetes Federation.
- Kokkinos, A. (2019). *Atlas of the diabetic foot, Third edition*. ed. Wiley Blackwell, Hoboken, New Jersey
- Lahiri, B.B., Bagavathiappan, S., Jayakumar, T., & Philip, J. (2012). Medical applications of infrared thermography: A review. *Infrared Physics & Technology* 55, 221–235. Available at: <https://doi.org/10.1016/j.infrared.2012.03.007> (Accessed: 19.04.2023)
- Lavery, L.A., Higgins, K.R., Lanctot, D.R., Constantinides, G.P., Zamorano, R.G., Athanasiou, K.A., Armstrong, D.G., & Agrawal, C.M. (2007). Preventing Diabetic Foot Ulcer Recurrence in High-Risk Patients: Use of temperature monitoring as a self-assessment tool. *Diabetes Care* 30, 14–20. Available at: <https://doi.org/10.2337/dc06-1600> (Accessed: 20.04.2023)
- Lavery, L.A., Peters, E.J.G., & Bush, R.L. (2010). *High risk diabetic foot: treatment and prevention*. Informa Healthcare, New York. Available at: <https://doi.org/10.3109/9781420083026> (Accessed: 06.02.2023)
- Machin, G., Whittam, A., Ainarkar, S., Allen, J., Bevans, J., Edmonds, M., Kluwe, B., Macdonald, A., Petrova, N., Plassmann, P., Ring, F., Rogers, L., & Simpson, R. (2017). A medical thermal imaging device for the prevention of diabetic foot ulceration. *Physiological measurement* 38, 420–430. Available at: <https://doi.org/10.1088/1361-6579/aa56b1> (Accessed: 05.04.2023)
- Meola, C. (2012). *Infrared thermography recent advances and future trends*. Bentham Science Publishers Ltd, SAIF Zone. Available at: <https://doi.org/10.2174/97816080514341120101> (Accessed: 07.02.2023)
- Ring, E.F.J., & Ammer, K. (2012). Infrared thermal imaging in medicine. *Physiological measurement* 33, R33-R46. Available at: <https://doi.org/10.1088/0967-3334/33/3/R33> (Accessed: 19.04.2023)
- Ring, E.F.J., Jung, A., & Žuber, J. (2015). *Infrared imaging: a casebook in clinical medicine, IOP expanding physics*. IOP Publishing, Bristol, UK. Available at: <https://doi.org/10.1088/978-0->

7503-1143-4 (Accessed: 04.02.2023)

Ring, F. (2010). Thermal Imaging Today and Its Relevance to Diabetes. *Journal of Diabetes Science and Technology* 4, 857-862. Available at: <https://doi.org/10.1177/193229681000400414> (Accessed: 03.02.2023)

Rother, C., Kolmogorov, V., & Blake, A. (2004). "GrabCut": interactive foreground extraction using iterated graph cuts. *ACM Transactions on Graphics* 23, 309–314. Available at: <https://doi.org/10.1145/1015706.1015720> (Accessed: 14.02.2023)

Soo, B.P., Rajbhandari, S., Egun, A., Ranasinghe, U., Lahart, I.M., & Pappachan, J.M. (2020). Survival at 10 years following lower extremity amputations in patients with diabetic foot disease. *Endocrine* 69, 100–106. Available at: <https://doi.org/10.1007/s12020-020-02292-7> (Accessed: 05.04.2023)

Usamentiaga, R., Venegas, P., Guerediaga, J., Vega, L., Molleda, J., & Bulnes, F.G. (2014). Infrared Thermography for Temperature Measurement and Non-Destructive Testing. *Sensors* 14, 12305–12348. Available at: <https://doi.org/10.3390/s140712305> (Accessed: 19.04.2023)

Wijlens, A.M., Holloway, S., Bus, S.A., & van Netten, J.J. (2017). An explorative study on the validity of various definitions of a 2·2°C temperature threshold as warning signal for impending diabetic foot ulceration. *International wound journal* 14, 1346–1351. Available at: <https://doi.org/10.1111/iwj.12811> (Accessed: 20.04.2023)